Modified test for chloride permeability of alkali-activated concrete

Robert J. Thomas
Ph.D. Candidate
Department of Civil and Environmental Engineering
Clarkson University
8 Clarkson Ave, Box 5712
Potsdam, NY 13676, USA

Sulapha Peethamparan (corresponding author)
Associate Professor
Department of Civil and Environmental Engineering
Clarkson University
8 Clarkson Ave, Box 5710
Potsdam, NY 13676, USA

4600 words + 8 figures + 2 tables

July 30, 2015

ABSTRACT
The resistance of concrete to chloride ion penetration is one of the most important durability properties. The diffusion coefficient is the best measurement of chloride penetration resistance, but can only be determined from chloride ponding tests which may take several months to complete. Accelerated test methods like rapid chloride penetrability test (RCPT) and bulk resistivity have proven effective in rapidly estimating chloride penetration resistance in portland cement concrete. These methods effectively measure the electrical properties of concrete, which are sensitive to the porosity and the conductivity of the pore solution. Due to the high ionic concentration in alkali-activated concrete (AAC), electrical test methods like RCPT and bulk resistivity may result in unsafely high electrical currents at worst or misleading results at best. This paper discusses the results and interpretation of such electrical test methods for AAC and investigates modifications to the RCPT procedure which may improve its applicability to AAC. The results indicate that increasing the RCPT specimen length from 51 mm to 153 mm reduces the electrical current to safe levels. The initial current and cumulative charge vary approximately linearly with specimen length, and the results show excellent agreement with bulk resistivity and porosity data.

INTRODUCTION

Measurement of chloride penetrability

The chloride diffusion into concrete is commonly modeled by Fick's First Law (Equation 1) for steady state conditions or Fick's Second Law (Equation 2) for non-steady state, where J is the chloride (or other) ion flux, D is the diffusion coefficient, $\phi(x)$ is the concentration gradient, and x is distance (1–5).

$$J = -D\frac{\partial \phi}{\partial x} \tag{1}$$

$$\frac{\partial \phi}{\partial t} = D\frac{\partial^2 \phi}{\partial x^2} \tag{2}$$

The diffusion coefficient D is a measure of the rate at which ions diffuse into the concrete. Hence, a low diffusion coefficient corresponds to concrete that is highly resistant to chloride penetration. The diffusion coefficient changes with the degree of saturation and with the pore structure; the latter is in turn affected by the characteristics of the binder, the degree of hydration, and the presence of microcracking (1–5). The concentration gradient $\phi(x)$ describes the total chloride concentration C_t at a distance x from the surface. This chloride exists in a form which is chemically or physically bound to the concrete matrix (bound chloride, C_b) and free chloride C_f, where only free chlorides are related to the corrosion of steel reinforcement (2, 4).

The 90-day salt ponding test (AASHTO T259/ASTM C1543) (6, 7) is unquestionably the best method of predicting the chloride permeability of concrete because, in conjunction with profile grinding and free chloride analysis, the salt ponding test can give the effective chloride diffusion coefficient D from Equations 1 and 2. However, the test requires 28 days curing, 14 days drying, 90 days ponding, and time-consuming titration analyses to determine free and total chloride concentrations at various location; this can require as long as six months for test results.

Due to the long duration of the salt ponding test, several accelerated methods are commonly used to predict the resistance of concrete to chloride penetration. The AASHTO T277/ASTM C1202 (8, 9) rapid chloride permeability test (RCPT) makes use of an electrochemical cell with an applied electric field, where current flow is taken as an indicator of chloride ion migration. Although commonly used in the literature, RCPT is not without limitations. Primarily, the measured current is an indication of the flow of all ions, not just chlorides. It is known that concrete with highly conductive pore solutions or high ionic concentrations result in spuriously high current readings which may not be indicative of poor resistance to chloride penetration (9**?**) Additionally, high currents tend to increase the temperature, further accelerating ion migration. For safety, most RCPT instruments limit current to 500 mA. Finally, RCPT results represent non-steady state ion migration. RCPT results are known to have a high degree of uncertainty, and are therefore used only qualitatively.

The bulk electrical resistivity of concrete is also frequently used as an indicator of chloride penetration resistance, where high resistivity is an indicator of high chloride penetration resistance. Both alternating and direct current measurements of resistivity are possible, although the latter introduces high uncertainties due to polarization. With regard to electrical properties, concrete is considered in two phases: Highly resistive concrete matrix and highly conductive pore solution. Since the conductivity of the matrix is negligible, the flow of electrical current through concrete depends on the pore structure and on the conductivity of the pore solution (3, 10, 11). Assuming

similar pore solution conductivity, higher porosity results in lower resistivity; it logically follows that a more porous concrete is also less resistant to chloride penetration. However, assuming similar pore structure, an increase in pore solution conductivity also results in lower resistivity, but is not likely to affect the chloride penetration resistance.

Finally, since the diffusion coefficient D is related to the porosity and pore structure within the concrete matrix, the porosity can be taken as a rudimentary indicator of resistance to chloride penetration, where decreased porosity indicates increased chloride penetration resistance. This may only be taken as a rudimentary indication since the porosity describes only the volume of pores and not the pore connectivity, pore size distribution, or tortuosity; all of these affect chloride ion migration.

Alkali-activated concrete (AAC)

Clinkerless binders for concrete made by the alkali-activation of ground granulated blast-furnace slag (GGBFS) and fly ashes have recently emerged as promising sustainable alternatives to ordinary portland cement (OPC). The benefits of these binders are mainly related to the associated emissions and embodied energy. Production of one tonne of ordinary portland cement (OPC) requires about 4 GJ of energy, mainly from fossil fuel sources, and results in as much as 0.95 tonnes of CO_2 emissions, contributing 5–7% of global anthropogenic carbon emissions (12–14). Recent studies have suggested considerable reductions in both the carbon emissions and embodied energy associated with the use of alkali-activated concrete, all at comparable costs to OPC concrete (15–19).

Volumes of studies are available which characterize the product formation, microstructure development, reaction kinetics, and mechanical properties of alkali-activated fly ash (AAF) and GGBFS (AAS) binders and concrete. A recent handbook has neatly summarized the state of the art in this area (20). The durability of such binders and concrete has also been widely discussed, although fewer sound conclusions have been made to that regard (21).

The chloride penetration resistance of AAC has received much attention in particular. More than a decade ago, Shi (22) discussed the limitations of RCPT for use with non-OPC binders due to the effect of variations in pore solution chemistry. Nevertheless, the industry desires a rapid method of estimating the chloride penetration resistance of concrete made with such binders. Bernal et al. (23) discussed the chloride penetration resistance of AAS concrete, concluding that the chloride penetration resistance was superior to that typical of OPC concrete. Furthermore, that study suggested that there was poor correlation between the charge passed during RCPT and the chloride diffusion coefficient as a result of mobile alkalis in the pore solution (23). Chi (24) also evaluated the chloride penetration resistance of AAS concrete by RCPT, drawing similar conclusions. That study indicated that the transport of free alkalis present in the pore solution of AAC lead to spuriously high charges passed during RCPT which are not necessarily indicative of chloride transport (24).

Fewer studies are available which have discussed the chloride penetration resistance of AAF concrete. Adam (25) performed RCPT for AAF concrete, and found that the initial current was very high compared to that in AAS concrete. The current continued to increase rapidly to unsafe levels as a result of the aforementioned temperature effects. That study also found good correlation between the electrical conductivity (the reciprocal of resistivity ρ) and charge passes during RCPT for AAF and AAS concrete. Further, it was again suggested that the high currents and charges recorded in AAF concrete were not directly indicative of very poor resistance to chloride

TABLE 1 : Mixture proportions (P: portland cement, F: class C fly ash, S: GGBFS, *: mixture also tested under heat-curing)

ID	$\%Na_2O$ (binder mass)	m	$\%SiO_2$ (binder mass)	s/b (by mass)	Solution (kg/m^3)	Binder (kg/m^3)	Fine Aggr (kg/m^3)	Coarse Aggr (kg/m^3)
P1	—	—	—	0.40	228	570	658	780
F1	4.0	1.5	6.0	0.40	228	570	658	780
F2*	5.0	1.5	7.5	0.40	228	570	658	780
S1	4.0	1.5	6.0	0.40	228	570	658	780
S2*	5.0	1.5	7.5	0.40	228	570	658	780
S3	4.0	0.75	3.0	0.40	228	570	658	780
S4*	5.0	0.75	3.75	0.40	228	570	658	780

penetration (25). More recently, Adak et al. (26) studied the effect of nanoparticles on the durability properties of AAF concrete, also recording high cumulative charges during RCPT. That discussion led to the assertion that, for AAC, RCPT may be more useful as a comparative tool for mixtures with similar pore solution chemistry rather than a qualitative or quantitative tool.

Objectives

This study investigates the chloride penetration resistance of AAC using electrical resistivity and modified RCPT. The effect of specimen length on the cumulative charge during RCPT is evaluated in an attempt to specify a more appropriate specimen length for evaluating the chloride penetration resistance of AAC by RCPT. The results of such tests are disseminated in the context of existing literature, and the interpretation of resulting data is discussed.

RESEARCH SIGNIFICANCE

The chloride-induced corrosion of steel in reinforced concrete is among the leading causes of infrastructure deterioration in the United States. The chloride permeability of concrete is therefore one of the most significant factors in determining the long-term durability of structural concrete. Due to the long duration of the AASHTO T259/ASTM C1543 (6, 7) salt ponding test, a rapid test method is preferred. However, the high ionic conductivity of the pore solution in alkali-activated concrete renders results from the AASHTO T277/ASTM C1202 (8, 9) rapid chloride permeability test (RCPT) unreliable. A modified test method which can rapidly and reliably predict the chloride permeability of alkali-activated concrete is therefore immediately necessary. This paper discusses the development of such a method and the analysis of the resulting data.

EXPERIMENTAL INVESTIGATION

Materials

The binders used in this study were ASTM C150 compliant Type-I ordinary portland cement (OPC), ASTM C618 compliant Class-C coal fly ash (FC), and ASTM C989 compliant Grade-100 ground granulated blast-furnace slag (GGBFS). The mixtures tested included one portland cement control mixture, two alkali-activated fly ash mixtures, and six alkali-activated GGBFS mixtures. One fly ash mixture and two GGBFS mixtures were selected to evaluate the effect of heat-curing. The mixture proportion details are shown in Table 1.

Specimen preparation and curing

Specimens were cast in the standard manner in accordance with the specifications of ASTM C192 (27). The alkaline activator was prepared in advance using reagent-grade sodium metasilicate solution, sodium hydroxide beads, and deionized water. Concrete was mixed by hand to provide the most homogeneous mixtures possible. Specimens were cast in appropriate molds (either 100 x 200 mm cylinders or 300 x 100 mm disks), consolidated on a vibrating table, sealed, and stored in a moist-curing room at 22±2 °C and greater than 95 %RH for 28 days. Alternatively, some specimens were heat-cured at 50±0.1 °C for 48 hours.

Test methods

Absorption capacity and permeable porosity of concrete cylinders measuring 100 mm in diameter and 200 mm in length was determined by the saturation method in general accordance with the specifications of ASTM C642 (28), except that vacuum saturation was used in lieu of cold water or boiling water saturation after Safiuddin and Hearn (29). The absorption capacity A was found from Equation 3, where W_s is the saturated unit weight and W_d is the oven-dried unit weight. Similarly, the permeable porosity P was determined from Equation 4, where W_b is the buoyant unit weight.

$$A = \frac{W_s - W_d}{W_d} \tag{3}$$

$$P = \frac{W_s - W_d}{W_s - W_b} \tag{4}$$

RCPT was performed in accordance with the specifications of AASHTO T277 and ASTM C1202 (8, 9) in the configuration shown in Figure 1. The maximum current was 500 mA, above which the power supply was automatically interrupted for safety reasons. The test duration was six hours and the applied voltage was 60 V. The specimen diameter was 102 mm and the length was varied between 51 and 153 mm.

The bulk resistivity of concrete cylinders measuring 100 mm in diameter and 200 mm in length was measured by AC impedance in the configuration shown in Figure 2. Alternating current in with frequency f of 1.0 kHz was applied across opposing cylinder end faces by two electrode plates with conductive sponges. The bulk resistivity is calculated from Equation 5, where R is the resistance, A_c is the cross-sectional area of the cylinder and ℓ is the cylinder length.

$$\rho = R\frac{A_c}{\ell} \tag{5}$$

RESULTS AND DISCUSSION

The bulk resistivity and permeable porosities of the tested concrete mixtures are presented in Figure 3. The porosities of OPC and AAS concrete were comparable, but those of AAF concrete were at least 50% higher. The prevalence of microcracking in AAF concrete—particularly if heat-curing is employed—has been reported elsewhere (30) and is a likely reason for the high porosity observations reported here. The resistivity of AAF concrete was about half that of OPC concrete; that of AAS concrete was an order of magnitude higher than either OPC or AAF. As expected, the resistivity was inversely related to the porosity. The resistivity observed for AAS concrete is extremely high, although at least one other study has observed resistivity values in AAS concrete that were much higher than in OPC concrete (31).

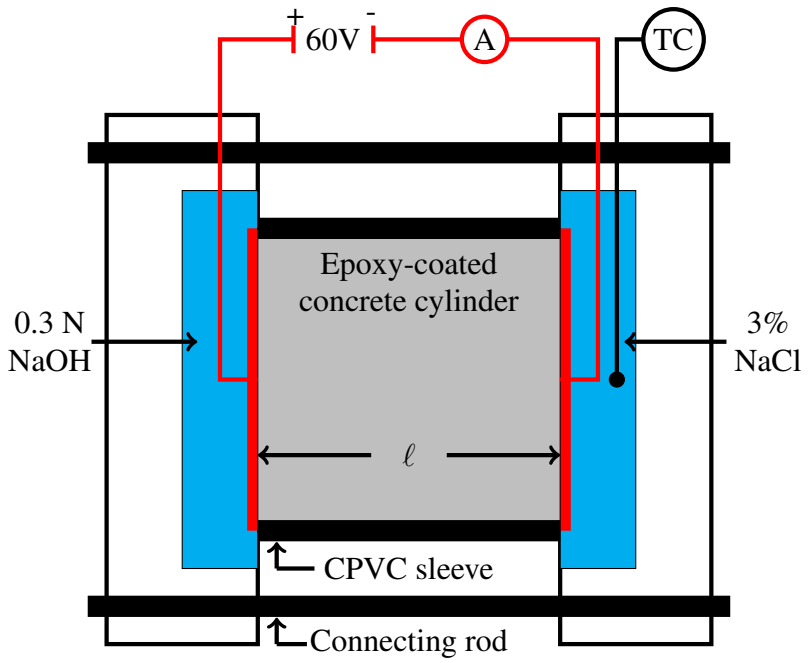

FIGURE 1 : Rapid chloride permeability test (ℓ is the specimen length)

Several representative RCPT results are plotted in Figures 4– 8. These results, as well as those for porosity and resistivity, are also summarized in Table 2. The values reflect the average of two replicates for RCPT and three replicates for resistivity and permeable porosity. OPC concrete (Figure 4) performed as expected; after some initial warm-up, the current was generally stable and the cumulative charge increased monotonically accompanied by a moderate temperature increase. The current, cumulative charge, and temperature increase diminished as the specimen length ℓ increased. With ℓ=153 mm, the temperature increase was limited to about 3 °C and the cumulative charge in 6 h was nearly halved compared to that observed when ℓ=51 mm. AAS concrete (Figure 5) performed similarly to OPC concrete; at all ℓ, the temperature increase was slightly higher than in OPC concrete despite lower current and charge. The reduction in current and charge as ℓ increased was more significant in AAS concrete than in OPC, and in some cases a factor of four reduction was realized by tripling ℓ from 51 mm to 153 mm.

The unmodified RCPT proved useful for AAS concrete and, following the test specifications (8, 9), most AAS mixtures were classified as having moderate or good resistance to chloride penetration. This was accompanied by very low porosity—some less than 5%—and extremely high electrical resistivity. Heat-curing resulted in increased electrical resistivity, decreased porosity, and decreased cumulative charge during RCPT. Heat-curing is known to result in a more refined microstructure in AAS concrete, and so it logically follows that the porosity and chloride penetration resistance would improve in turn. The solution concentration (sodium oxide concentration and silica modulus m) had a varied effect on porosity and resistivity. However, the cumulative charge during RCPT decreased as the silica modulus m increased and as the sodium oxide concentration increased. Both are also known to improve the mechanical properties of AAS concrete, and so this result also logically follows.

RCPT for AAF concrete was plagued with difficulties. This is shown in Figures 6– 8,

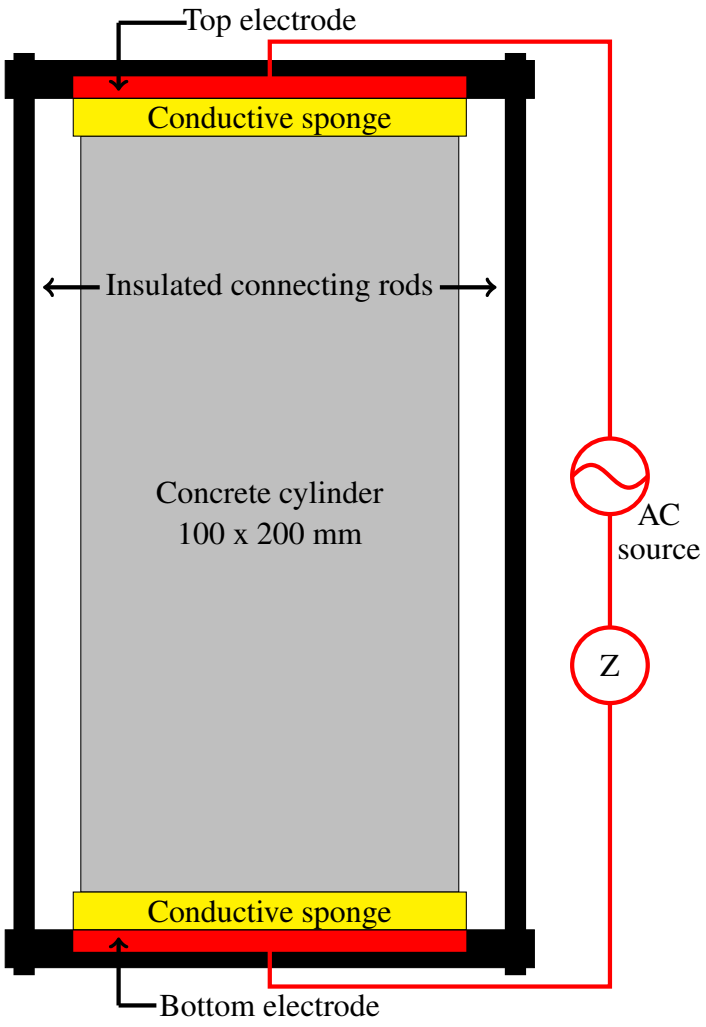

FIGURE 2 : Bulk electrical impedance test

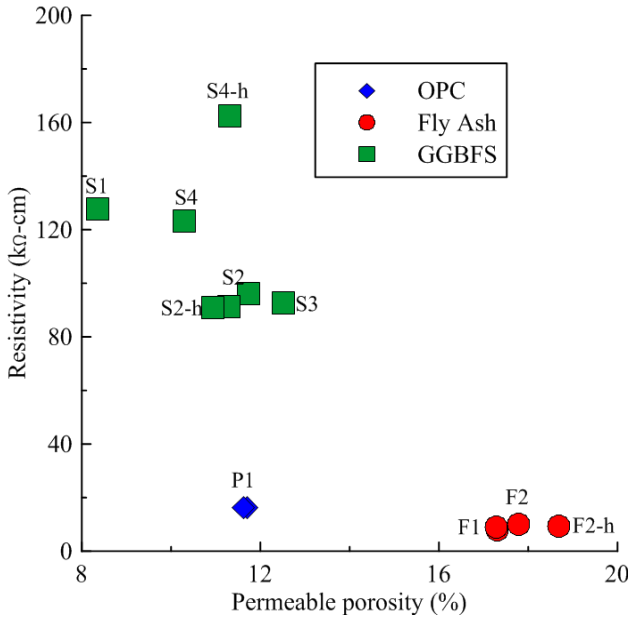

FIGURE 3 : Resistivity v. porosity for AAC and OPC mixtures

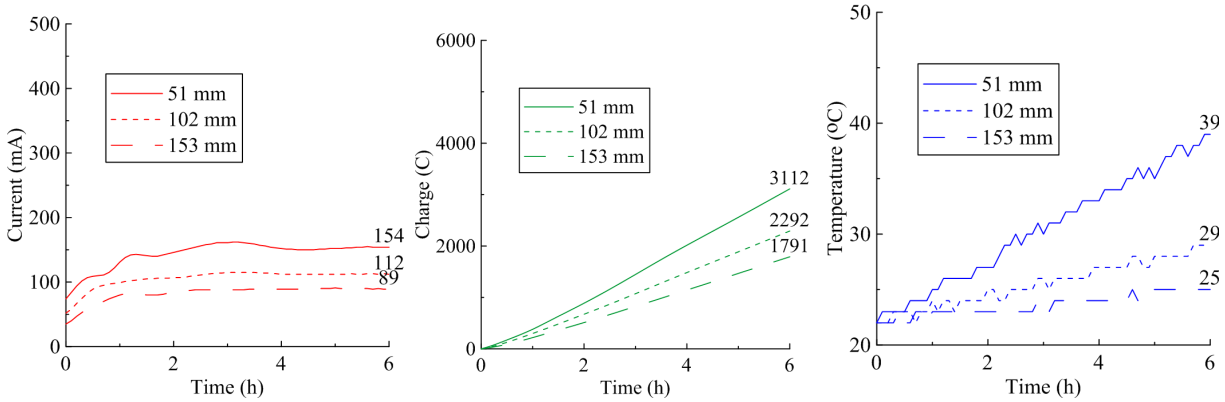

(a) Current (b) Charge (c) Temperature

FIGURE 4 : RCPT data for OPC concrete mixture P1 with $\ell = \{51, 102, 153\}$ mm

TABLE 2 : Resistivity ρ, porosity P, and RCPT results

Mix	ℓ (mm)	ρ (kΩ-cm) [200 mm]	P (%)	Initial current (mA)	Cumulative charge (C) 30 m	1 h	6 h
P1	51			74	173	380	3112
P1	102	16.4	11.7	52	127	298	2292
P1	153			35	89	219	1791
F1	51			>500	*immediately over limit*		
F1	102	8.0	17.3	387	572	(*after 0.4 h*)	
F1	153			312	745		
F2	51			478	275	(*after 0.2 h*)	
F2	102	9.9	17.9	332	747		
F2	153			295	625	1392	
F2-h	51			395	436	(*after 0.3 h*)	
F2-h	102	17.6	10.0	314	663		
F2-h	153			271	587	1395	
S1	51			99	209	432	3774
S1	102	128	3.6	56	118	250	1914
S1	153			21	46	104	962
S2	51			76	148	317	2635
S2	102	96	5.0	39	99	220	1581
S2	153			15	37	87	742
S2-h	51			82	160	339	2559
S2-h	102	91	4.8	39	99	220	1581
S2-h	153			17	39	98	869
S3	51			63	131	277	2430
S3	102	93	12.5	23	53	120	1038
S3	153			7	23	60	636
S4	51			61	117	256	2016
S4	102	123	10.3	17	43	101	828
S4	153			7	17	46	518
S4-h	51			49	100	230	1814
S4-h	102	162	5.0	14	38	95	784
S4-h	153			3	14	42	442

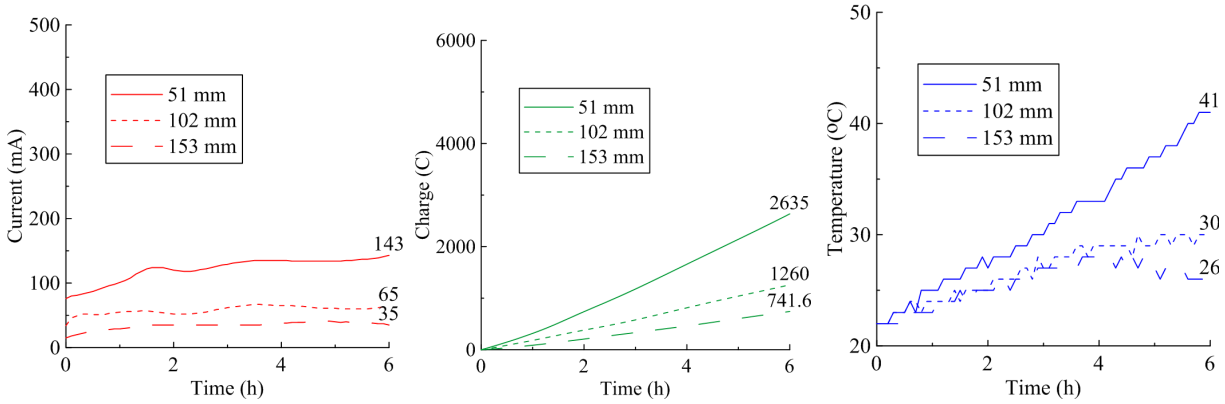

(a) Current (b) Charge (c) Temperature

FIGURE 5 : RCPT data for AAS concrete mixture S2 with $\ell = \{51, 102, 153\}$ mm

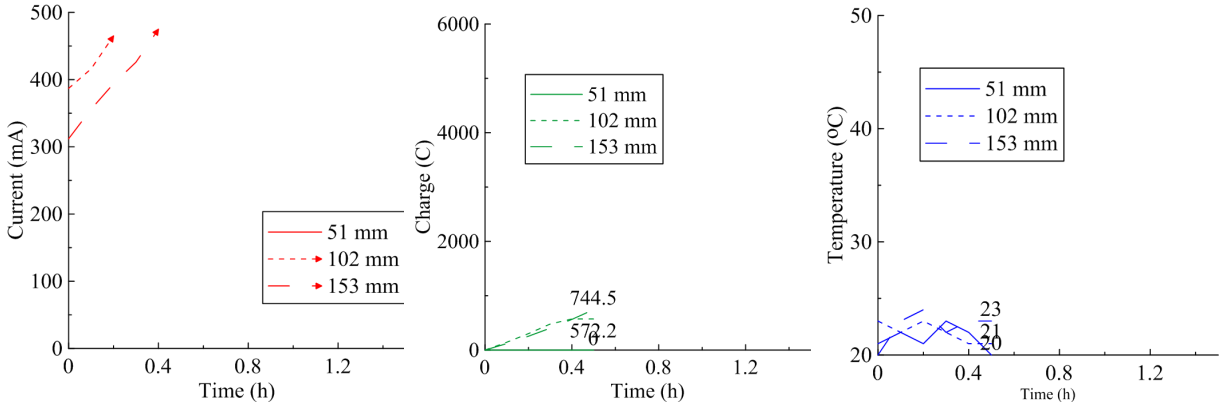

(a) Current (b) Charge (c) Temperature

FIGURE 6 : RCPT data for AAF concrete F1 with $\ell = \{51, 102, 153\}$ mm

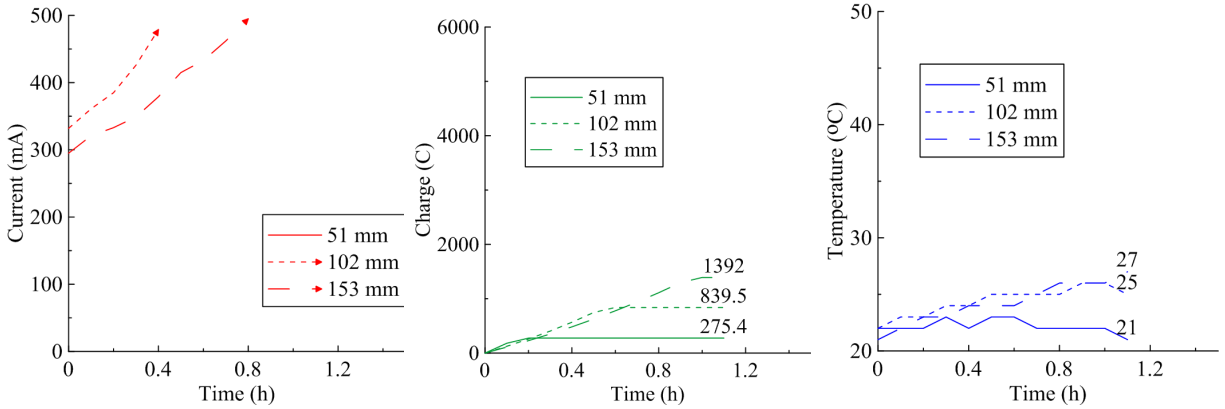

(a) Current (b) Charge (c) Temperature

FIGURE 7 : RCPT data for AAF concrete F2 with $\ell = \{51, 102, 153\}$ mm

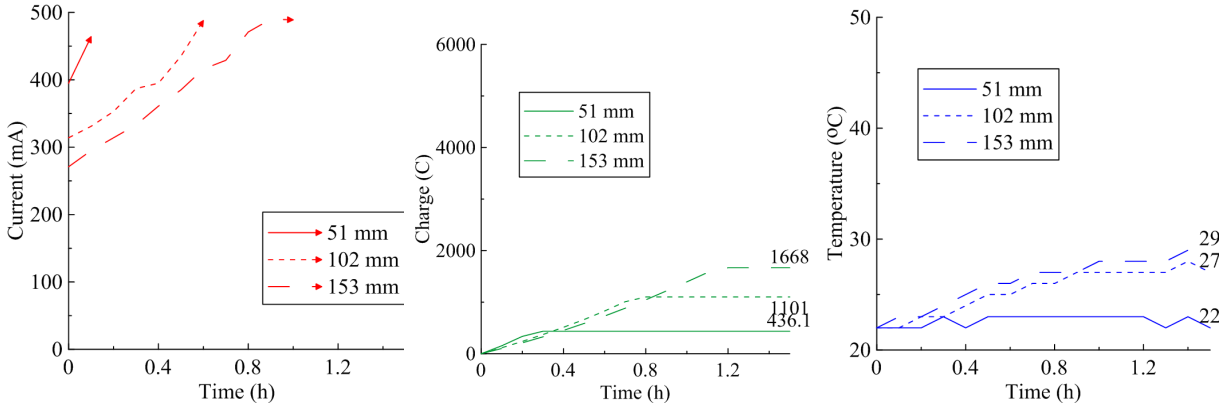

(a) Current (b) Charge (c) Temperature

FIGURE 8 : RCPT data for AAF concrete F2 (heat-cured) with $\ell = \{51, 102, 153\}$ mm

where the test was stopped prematurely as the current exceeded the 500 mA safe limit. In most cases, the initial current exceeded the safe limit with ℓ=51 mm. As ℓ increased to 102 mm and 153 mm, the initial current was reduced to safe levels, but rapidly increased and exceeded the limit in quick succession. In most cases, the current limit was exceeded within 30 minutes when ℓ=102 mm and soon after 1 hour when ℓ=153 mm. Even with limited data, however, it can be observed that the specimen length affected the initial current and the cumulative charge for AAF concrete in a similar manner as for AAS and OPC concrete, allowing for some limited comparisons based on extrapolation. The initial current in AAF concrete was about five times that in AAS concrete, and the cumulative charge after 30 minutes was 2–3 times higher. For those specimens that remained under the current limit after one hour, the cumulative charge was a full order of magnitude higher in AAF concrete than in AAS. This clearly shows the superiority of AAS concrete to AAF in terms of chloride penetrability. Extrapolating from the limited data available would suggest that the total charge after six hours in AAF concrete, were it possible to measure by traditional RCPT methodology, would be of the order 10^5 C.

The porosity of AAF concrete mixtures was very high—more than 15%—and the electrical resistivity was very low—about half that of OPC concrete. This, in addition to the very high current during RCPT, suggests that the chloride penetration resistance of AAF concrete is poor, especially relative to that of AAS concrete. The high porosity could be at fault for the poor resistance to chloride penetration, and may be a result of the microcracking which is known to occur in alkali-activated concrete. However, microcracking is supposed to be more prevalent in heat-cured mixtures; here the porosity was reduced under heat-curing, as was the chloride penetration resistance. As with AAS concrete, heat-curing is known to improve the microstructure and mechanical properties of AAF concrete, and so it is reasonable that the resistance to chloride penetration would also be improved.

A known problem with RCPT is that it measures the transport of all ions. Alkali-activated concrete has a very high ionic concentration compared to OPC concrete. This implies that, taken at face value, the RCPT results would offer a conservative estimate of the chloride penetration resistance of AAC. For AAS concrete, this means that the chloride penetration resistance is moderate at worst. The very high resistivity and very low porosity of said AAS concrete would suggest even better resistance. For AAF concrete, even though the current and porosity are high and the

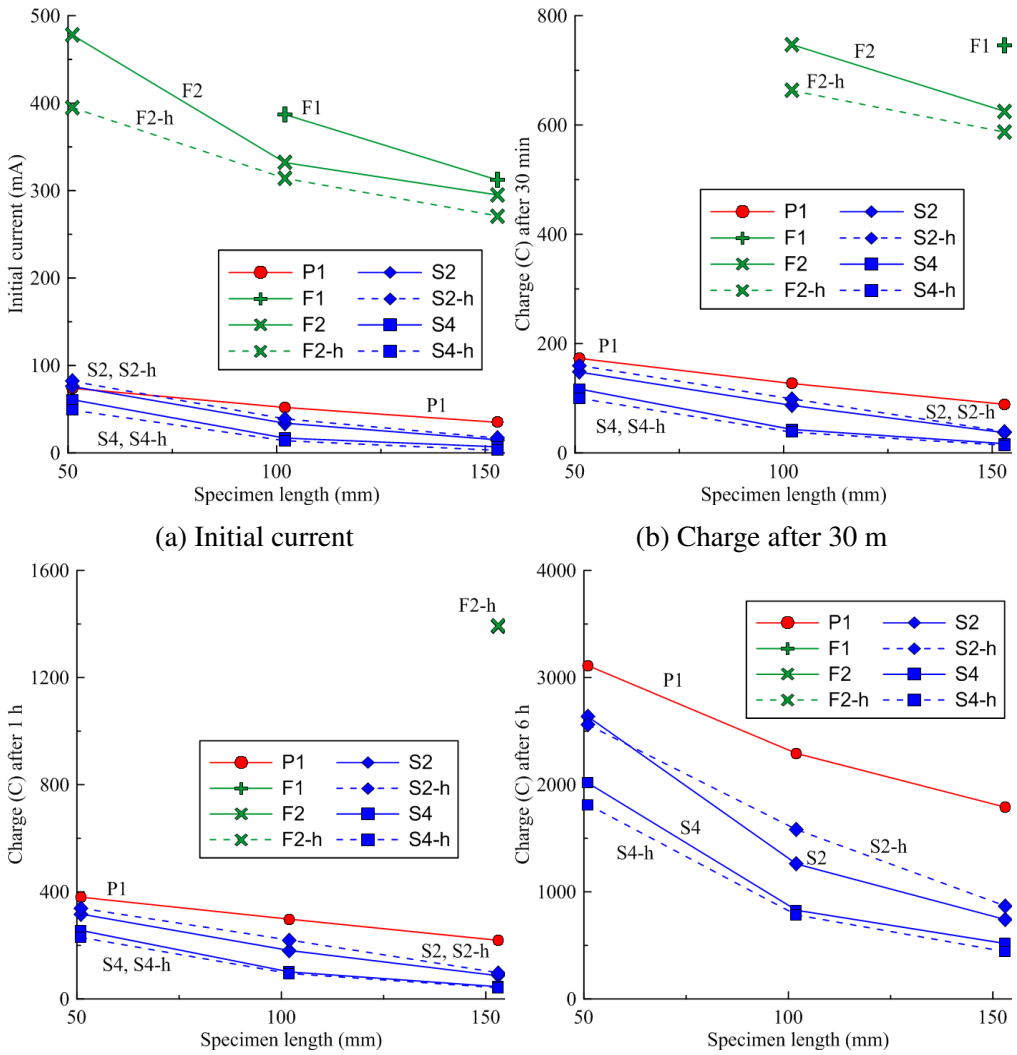

(a) Initial current (b) Charge after 30 m

(c) Charge after 1 h (d) Charge after 6 h

FIGURE 9 : RCPT initial current and charge passed after $\{0.5, 1, 6\}$ h for OPC, AAS, and AAF concrete with $\ell = \{51, 102, 153\}$ mm

resistivity is low, the chloride penetration may not be as poor as indicated. In reality, it is necessary to perform salt ponding tests and calculate the actual diffusion coefficient D from Fick's Law (Equations 1 and 2) to draw sound conclusions. This would allow the calibration of the modified RCPT for AAS and AAF concrete.

CONCLUSIONS

This study was performed to evaluate electrical methods of predicting the resistance of AAC to penetration by chlorides, and to investigate modifications to such test methods to overcome test complications resulting from high ionic concentrations in AAC. The following general conclusions are drawn from the results of this study:

- AAS concrete exhibits low porosity, very high electrical resistivity, and low current during RCPT, suggesting that AAS concrete may be highly resistant to chloride ion penetration
- AAF concrete exhibits high porosity, very low electrical resistivity, and high current during RCPT, suggesting that AAF concrete may be poorly resistant to chloride ion penetration
- Heat-curing reduces porosity and increases chloride penetration resistance for both AAF and AAS concrete
- The exceptionally high current and temperature increase in AAF concrete during RCPT may be effectively reduced to safe and measurable levels by increasing the specimen length from 51 mm to 102 or 153 mm
- Despite reducing the initial current in AAF during RCPT by increasing specimen length, the heating effects still increase the current flow above the safe limit within an hour
- The initial current during RCPT correlates well to the cumulative charge after various time steps, suggesting that the initial current may be a good indicator of chloride penetration resistance when the over-current limit is exceeded before 6 h

The results of this study have significant implications for durability testing of AAC, although the results must be further qualified through continued experimentation. Primarily, a better understanding of the electrical properties of AAC may be achieved by studying the properties of the pore solution and by more advanced analysis of the pore structure. Furthermore, the RCPT and bulk resistivity results presented here should be compared to chloride diffusion coefficients determined from salt ponding tests.

ACKNOWLEDGMENTS

Funding for this research was provided by the University Transportation Research Center, Region 2 (UTRC2) and by the National Science Foundation under CMMI Award No. 1055641.

REFERENCES

[1] Andrade, C., Calculation of chloride diffusion coefficients in concrete from ionic migration measurements. *Cem Concr Res*, Vol. 23, No. 3, 1993, pp. 724–742.

[2] Saetta, A. V., R. V. Scotta, and R. V. Vitaliani, Analysis of chloride diffusion into partially saturated concrete. *ACI Mater J*, Vol. 90, No. 5, 1993.

[3] Stanish, K., R. Hooton, and M. Thomas, Testing the chloride penetration resistance of concrete: A literature review. *FHWA contract DTFH61*, 1997, pp. 19–22.

[4] Xi, Y. and Z. Bazant, Modeling chloride penetration in saturated concrete. *J Mater Civil Engr*, Vol. 11, No. 1, 1999, pp. 58–65.

[5] Thomas, M. D. and P. B. Bamforth, Modelling chloride diffusion in concrete: effect of fly ash and slag. *Cem Concr Res*, Vol. 29, No. 4, 1999, pp. 487–495.

[6] AASHTO T259-02, Standard Test Method for Resistance of Concrete to Chloride Ion Penetration. *AASHTO*, 2012.

[7] ASTM C1543-10, Standard Test Method for Determining the Penetration of Chloride Ion into Concrete by Ponding. *ASTM Int*, 2010.

[8] AASHTO T277-07, Standard Test Method for Electrical Indication of Concrete's Ability to Resist Chloride Ion Penetration. *AASHTO*, 2012.

[9] ASTM C1202-12, Standard Test Method for Electrical Indication of Concrete's Ability to Resist Chloride Ion Penetration. *ASTM Int*, 2012.

[10] Kyi, A. A. and B. Batchelor, An electrical conductivity method for measuring the effects of additives on effective diffusivities in Portland cement pastes. *Cem Concr Res*, Vol. 24, No. 4, 1994, pp. 752–764.

[11] Streicher, P. and M. Alexander, A chloride conduction test for concrete. *Cem Concr Res*, Vol. 25, No. 6, 1995, pp. 1284–1294.

[12] Worrell, E., N. Martin, and L. Price, Potentials for energy efficiency improvement in the US cement industry. *Energy*, Vol. 25, No. 12, 2000, pp. 1189–1214.

[13] van Oss, H. and A. Padovani, Cement manufacture and the environment. *Journal of Industrial Ecology*, Vol. 6, No. 1, 2002, pp. 89–106.

[14] Madlool, N., R. Saidur, M. Hossain, and N. Rahim, A critical review on energy use and savings in the cement industries. *Renewable and Sustainable Energy Reviews*, Vol. 15, No. 4, 2011, pp. 2042–2060.

[15] Duxson, P., J. Provis, G. Lukey, and J. Van Deventer, The role of inorganic polymer technology in the development of 'green concrete'. *Cem Concr Res*, Vol. 37, No. 12, 2007, pp. 1590–1597.

[16] van Deventer, J., J. Provis, R. Duxson, and D. Brice, Chemical research and climate change as drivers in the commercial adoption of alkali activated materials. *Waste and Biomass Valorization*, Vol. 1, No. 1, 2010, pp. 145–155.

[17] McLellan, B., R. Williams, J. Lay, A. Van Riessen, and G. Corder, Costs and carbon emissions for geopolymer pastes in comparison to ordinary portland cement. *J Clean Prod*, Vol. 19, No. 9, 2011, pp. 1080–1090.

[18] Yang, K., J. Song, and K. Song, Assessment of CO_2 reduction of alkali-activated concrete. *J Clean Prod*, Vol. 39, 2013, pp. 265–272.

[19] Turner, L. and F. Collins, Carbon dioxide equivalent (CO_2-e) emissions: a comparison between geopolymer and OPC concrete. *Constr Build Mater*, Vol. 43, 2013, pp. 125–130.

[20] Pacheco-Torgal, F., J. Labrincha, C. Leonelli, A. Palomo, and P. Chindaprasit, *Handbook of Alkali-Activated Cements, Mortars and Concretes*. Elsevier, 2014.

[21] Pacheco-Torgal, F., Z. Abdollahnejad, A. Camões, M. Jamshidi, and Y. Ding, Durability of alkali-activated binders: A clear advantage over Portland cement or an unproven issue? *Constr Build Mater*, Vol. 30, 2012, pp. 400–405.

[22] Shi, C., Effect of mixing proportions of concrete on its electrical conductivity and the rapid chloride permeability test (ASTM C1202 or ASSHTO T277) results. *Cem Concr Res*, Vol. 34, No. 3, 2004, pp. 537–545.

[23] Bernal, S., R. de Gutiérrez, and J. Provis, Engineering and durability properties of concretes based on alkali-activated granulated blast furnace slag/metakaolin blends. *Constr Build Mater*, Vol. 33, 2012, pp. 99–108.

[24] Chi, M., Effects of dosage of alkali-activated solution and curing conditions on the properties and durability of alkali-activated slag concrete. *Constr Build Mater*, Vol. 35, 2012, pp. 240–245.

[25] Adam, A., *Strength and durability properties of alkali activated slag and fly ash-based geopolymer concrete*. Ph.D. thesis, RMIT University Melbourne, Australia, 2009.

[26] Adak, D., M. Sarkar, and S. Mandal, Effect of nano-silica on strength and durability of fly ash based geopolymer mortar. *Construction and Building Materials*, Vol. 70, 2014, pp. 453–459.

[27] ASTM C192-15, Standard Practice for Making and Curing Concrete Test Specimens in the Laboratory. *ASTM Int*, 2015.

[28] ASTM C642-13, Standard Test Method for Density, Absorption, and Voids in Hardened Concrete. *ASTM Int*, 2012.

[29] Safiuddin, M. and N. Hearn, Comparison of ASTM saturation techniques for measuring the permeable porosity of concrete. *Cem Concr Res*, Vol. 35, No. 5, 2005, pp. 1008 – 1013.

[30] Puertas, F., S. MartıÌĄnez-RamıÌĄrez, S. Alonso, and T. Vazquez, Alkali-activated fly ash/slag cements: strength behaviour and hydration products. *Cem Concr Res*, Vol. 30, No. 10, 2000, pp. 1625–1632.

[31] Song, H.-W. and V. Saraswathy, Studies on the corrosion resistance of reinforced steel in concrete with ground granulated blast-furnace slagâĂŤan overview. *J Haz Mater*, Vol. 138, No. 2, 2006, pp. 226–233.